

Accepted Manuscript



Liver proteomics of gilthead sea bream (*Sparus aurata*) exposed to cold stress

S. Ghisaura, D. Pagnozzi, R. Melis, G. Biossa, H. Slawski, S. Uzzau, R. Anedda, M.F. Addis

PII: S0306-4565(18)30549-7

DOI: <https://doi.org/10.1016/j.jtherbio.2019.04.005>

Reference: TB 2305

To appear in: *Journal of Thermal Biology*

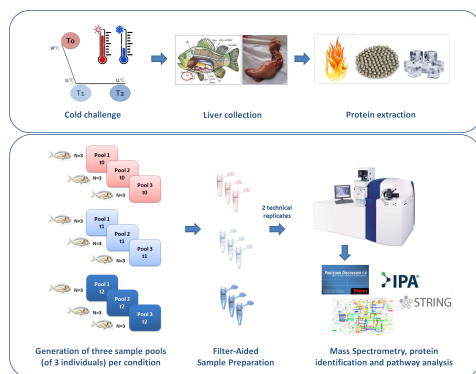
Received Date: 13 December 2018

Revised Date: 25 February 2019

Accepted Date: 12 April 2019

Please cite this article as: Ghisaura, S., Pagnozzi, D., Melis, R., Biossa, G., Slawski, H., Uzzau, S., Anedda, R., Addis, M.F., Liver proteomics of gilthead sea bream (*Sparus aurata*) exposed to cold stress, *Journal of Thermal Biology* (2019), doi: <https://doi.org/10.1016/j.jtherbio.2019.04.005>.

This is a PDF file of an unedited manuscript that has been accepted for publication. As a service to our customers we are providing this early version of the manuscript. The manuscript will undergo copyediting, typesetting, and review of the resulting proof before it is published in its final form. Please note that during the production process errors may be discovered which could affect the content, and all legal disclaimers that apply to the journal pertain.



ACCEPTED MANUSCRIPT

1 **Liver proteomics of gilthead sea bream (*Sparus aurata*) exposed to cold stress**

2

3 S. Ghisaura^{a§}, D. Pagnozzi^{a§}, R. Melis^a, G. Biosa^a, H. Slawski^b, S. Uzzau^{a,c}, R. Anedda^{a,**}, M.F. Addis^{a,d,*}

4 ^a Porto Conte Ricerche, Tramariglio, Alghero, Italy

5 ^b Aller Aqua, Christiansfeld, Denmark

6 ^c Department of Biomedical Sciences, University of Sassari, Italy

7 ^d Department of Veterinary Medicine, University of Milan, Italy

8

9

10

11 [§]These authors contributed equally

12 ^{*}Corresponding author. E-mail address: filippa.addis@unimi.it (M. F. Addis).

13 ^{**}Additional corresponding author. E-mail address: anedda@portocontericerche.it (R. Anedda).

14

15 **Short title: Cold stress and the sea bream liver proteome**

16

17 **Abstract**

18 The gilthead sea bream (*Sparus aurata*, L.) is very sensitive to low temperatures, which induce fasting and
19 reduced growth performances. There is a strong interest in understanding the impact of cold on fish
20 metabolism to foster the development and optimization of specific aquaculture practices for the winter
21 period. In this study, a 8 week feeding trial was carried out on gilthead sea bream juveniles reared in a
22 Recirculated Aquaculture System (RAS) by applying a temperature ramp in two phases of four weeks each:
23 a cooling phase from 18°C to 11°C and a cold maintenance phase at 11°C. Liver protein profiles were
24 evaluated with a shotgun proteomics workflow based on filter-aided sample preparation (FASP) and liquid
25 chromatography-mass spectrometry (LC-ESI-Q-TOF MS/MS) followed by label-free differential analysis.
26 Along the whole trial, sea breams underwent several changes in liver protein abundance. These occurred
27 mostly during the cooling phase when catabolic processes were mainly observed, including protein and lipid
28 degradation, together with a reduction in protein synthesis and amino acid metabolism. A decrease in protein
29 mediators of oxidative stress protection was also seen. Liver protein profiles changed less during cold
30 maintenance, but pathways such as the methionine cycle and sugar metabolism were significantly affected.
31 These results provide novel insights on the dynamics and extent of the metabolic shift occurring in sea bream
32 liver with decreasing water temperature, supporting future studies on temperature-adapted feed formulations.
33 The mass spectrometry proteomics data have been deposited to the ProteomeXchange Consortium via the
34 PRIDE partner repository with the dataset identifier PXD011059.

35

36 **Keywords: cold stress; winter syndrome; gilthead sea bream; liver proteins; methionine; shotgun**
37 **proteomics.**

38

39 1. Introduction

40 Gilthead sea breams (*Sparus aurata*, L.) have their natural habitat in the Mediterranean Sea at water
41 temperatures ranging seasonally from approximately 26°C in summer to 11-13°C or even lower in winter,
42 depending on the specific environment. Wild sea breams manage this temperature decrease by migrating to
43 deeper and warmer water (Davis, 1988). In fact, water temperatures below 13°C lead to both behavioral
44 (e.g., erratic swimming, voluntary fasting, hyposensitivity to stimuli) and physiological (e.g., impaired
45 growth, fatty liver, tissue necrosis, infections) stressful changes that can ultimately lead to physiological
46 dysfunction and death (Contessi et al., 2006; Gallardo et al., 2003; Ibarz et al., 2010b). However, farmed sea
47 breams living in outdoor tanks and in floating sea cages are unable to avoid this thermal stress, and their
48 prolonged exposure to temperatures below 13°C causes decrease in activity (Ibarz et al., 2003), growth delay
49 (Tort et al., 1998), metabolic depression (Ibarz et al., 2018; Sanahuja et al., 2019) and reduced feed
50 consumption until total fasting when water temperatures fall below 10°C (Ibarz et al., 2010b). Other
51 physiological alterations include hepatic functionality, with the liver becoming steatotic and whitish due to a
52 large deposition of lipids, as well as reduced efficiency of adaptive immunity with increased susceptibility to
53 infections (winter syndrome or winter disease) and alteration of the main redox pathways (Abram et al.,
54 2017; Ibarz et al., 2007, 2005; Sánchez-Nuño et al., 2018). These phenomena impact farming productions
55 causing relevant economic losses with a consequent strong interest of fish farmers in finding efficient
56 strategies for their reduction. One way for compensating thermal stress is represented by enhancing the
57 nutritional state and metabolism through the use of feeds specifically designed for the colder season, and this
58 requires understanding the consequences of cold on fish metabolism. To this aim, proteomic, metabolomic
59 and transcriptomic approaches have been applied to farmed and wild fish biofluids and tissues, such as
60 serum, liver, muscle and other organs, with differing degrees of success (Addis, 2013; Addis et al., 2010a,
61 2010b; Alves et al., 2010; Braceland et al., 2013; Brunt et al., 2008; Douxfils et al., 2011; Ghisaura et al.,
62 2014; Martin et al., 2001; Melis et al., 2017; Mininni et al., 2014; Rodrigues et al., 2012). Proteomics offers
63 several specific advantages when compared to genomic or transcriptomic strategies, including the ability to
64 evaluate the actual extent of protein abundance, going beyond the estimates based on gene expression. In
65 fact, proteins do not always follow a strict relationship with gene transcription but are regulated at the
66 translational or post-translational level. Liver, the main metabolic organ of the body, has gained the greatest

67 attention in proteomic studies evaluating the influence of farming practices on fish metabolism. Martin and
68 coworkers (Martin et al., 2001) studied the changes occurring in the liver proteome as a consequence of
69 different feeding regimens, including dietary plant protein substitution. Liver metabolism is considerably
70 influenced also by other factors including environmental stress, and might be affected by xenobiotics and
71 toxins (Addis, 2013; Ghisaura et al., 2014). Numerous research groups focused on the gilthead sea bream
72 liver proteome to investigate a variety of stressful factors, ranging from handling and crowding (Alves et al.,
73 2010) to the use of antiparasitic, or antibacterial agents and different environmental pollution (Isani et al.,
74 2011; Kovacik et al., 2018; Varó et al., 2013). Proteomics has also been used to assess the impact of cold on
75 fish metabolism (Ibarz et al., 2010a; Parrington and Coward, 2002; Vilhelmsson et al., 2003). However,
76 these studies applied a gel-based approach (2D-gel electrophoresis, 1D GelC-MS/MS). With the aim of
77 gathering additional information, we investigated the changes occurring in liver tissue by applying a shotgun
78 proteomics workflow based on filter-aided sample preparation (FASP), tandem mass spectrometry (MS/MS),
79 label-free quantitation and, finally, pathway analysis by means of STRING and Ingenuity Pathway Analysis
80 (IPA). In fact, this approach provides a higher proteome coverage and is less affected by the typical
81 limitations of gel-based studies, especially when 2D separation is involved (Westermeier et al., 2008), and
82 additional or complementary information can be obtained in respect to previous studies. Liver proteome
83 changes were assessed by mimicking the winter challenge conditions in a Recirculated Aquaculture System
84 (RAS), both immediately after temperature reduction and during cold maintenance.

85

86 **2. Materials and Methods**

87 **2.1. Experimental design**

88 A detailed description of the trial can be found in our previous work (Melis et al., 2017). For the purposes of
89 both studies, a total of 60 juvenile gilthead sea breams with an average weight of 82.0 ± 4.5 g were
90 uniformly distributed in three fiberglass tanks of 550 L with mechanical and biological filtration systems, a
91 pumping system, a water thermoregulation system, and an automatic control for adjusting and monitoring the
92 main physicochemical parameters. Fish were first acclimated for two weeks by linearly lowering water
93 temperature from 20°C to 18°C (t0). Then, temperature was reduced at a rate of approximately 1°C every
94 Tuesday and Friday until reaching 11°C (cooling phase, t0-t1, 4 weeks). Then, fish were maintained at 11°C

95 (cold maintenance phase, t1-t2) for the same time span (4 weeks). Fish were fed by hand, once a day, an
96 experimental feed formulation (Aller Aqua, Christiansfeld, Denmark) with 43% protein and 14% fat. Feed
97 ration was adjusted accounting for fish size, biomass and temperature (0.9 ± 0.03 g during cooling and $0.4 \pm$
98 0.03 g during cold maintenance). During the growth trial no mortality occurred, and fish never stopped
99 eating below 13°C. For the purposes of this study, at the beginning of the trial (t0) and at each time point (t1,
100 t2), 9 fishes were anesthetized with 1,1,1-trichloro-2-methylpropan-2-ol (2% in marine water) and
101 transferred in a mixture of marine water and ice (total number of sacrificed subjects = 27). Liver was excised
102 from each fish, weighed and frozen rapidly in liquid nitrogen in Petri dishes as described by Melis and
103 coworkers (2017).

104

105 **2.2. Protein extraction and quantification**

106 Fish liver protein extraction was performed according to Ghisaura et al. (2016). Briefly, a small portion of
107 each tissue (100 mg) was placed in a 2 ml Eppendorf safe-lock tube (Eppendorf, Hamburg, Germany) and
108 immersed at 25% w/v in lysis buffer (7 M urea, 2 M Thiourea, 2% CHAPS) plus protease inhibitor cocktail
109 (Protease Inhibitor Cocktail for General Use, Sigma-Aldrich, Saint Louis, MO) as indicated in the
110 manufacturer instructions. Samples were then processed and subjected to three cycles of 5 min at 30
111 oscillations/s in a TissueLyser mechanical homogenizer (Qiagen, Hilden, Germany). Samples were frozen in
112 between homogenization cycles to ease tissue disruption and avoid excessive sample heating. Protein
113 extracts were then centrifuged for 15 min at 18,000 x g at 4°C, quantified with the Pierce 660 nm Protein
114 Assay Kit (Thermo Scientific - Rockford, IL), evaluated for quality and integrity by SDS-PAGE (data not
115 shown), and stored at -80°C until use.

116

117 **2.3. Shotgun proteomics**

118 Three protein samples for each time point (t0, t1, t2), each constituted by a biological pool of three fish
119 liver extracts, were used for shotgun proteomics analysis. Protein extracts (n = 9) were subjected to on-
120 filter reduction, alkylation, and trypsin digestion according to the filter-aided sample preparation (FASP)
121 protocol (Wiśniewski et al., 2009), with minor modifications (Ghisaura et al., 2016; Tanca et al., 2013)
122 using Amicon Ultra-0.5 centrifugal filter units with Ultracel-10 membrane (Millipore, Billerica, MA,

123 USA). Peptide mixture concentration was estimated by using BCA protein assay kit (Thermo Scientific -
 124 Rockford, IL). LC-MS/MS analyses were performed on a Q-TOF hybrid mass spectrometer with a nano
 125 lock Z spray source, coupled on-line with a NanoAcquity chromatography system (Waters) (Pagnozzi et
 126 al., 2014). Two technical replicates were analyzed for each biological pool (total LC-MS/MS runs = 18).
 127 Peptide mixtures were concentrated and washed with an enrichment column and then fractionated over a
 128 250 min gradient on a C18 reverse phase column. The instrument was set up in a data-dependent MS/MS
 129 mode, with a full-scan spectrum followed by tandem mass spectra, selecting peptide ions as the three most
 130 intense peaks of the previous scan. ProteinLynx software (Version 2.2.5), was used to produce the peak
 131 lists as pkl files.

132

133 **2.4. Protein identification and differential proteomic analysis by label-free quantitation**

134 The Q-TOF peak lists were analyzed by Proteome Discoverer software (version 1.4; Thermo Scientific),
 135 after conversion into MGF files. Technical replicates were processed as merged, generating one list of
 136 identified proteins for each biological sample by the Proteome Discoverer Daemon utility. The workflow
 137 was made up of the following nodes (and respective parameters). Spectrum Selector for spectra pre-
 138 processing (precursor mass range: 350–5000 Da; S/N Threshold: 1.5), Sequest-HT as search engine
 139 (Protein Database: Chordata sequences from UniProtKB; Enzyme: Trypsin; Max. missed cleavage sites: 2;
 140 Peptide length range 5–50 amino acids; Max. Delta Cn: 0.05; Precursor mass tolerance: 50 ppm; Fragment
 141 mass tolerance 0.4 Da; Static modification: cysteine carbamidomethylation; Dynamic modification:
 142 methionine oxidation), and Percolator for peptide validation (FDR < 1% based on peptide q-value) (Choi
 143 and Nesvizhskii, 2008; Käll et al., 2009, 2008; Spivak et al., 2009). In order to estimate the extent of
 144 differential protein abundance among sample groups, the Normalized Spectral Abundance Factor (NSAF)
 145 was calculated for each protein according to Zybaylov et al. (Zybaylov et al., 2006) as follows:

146 $NSAF = SAF_i / \sum_{i=1}^N SAF_i$, where subscript i indicates a protein identity, N represents the total number of
 147 proteins, and SAF is a protein spectral abundance factor (protein spectral counts divided by its length).

148 Finally, the NSAF log ratio (R_{NSAF}) was calculated as follows: $R_{NSAF} = \log_2(NSAF_x + CF)/(NSAF_y + CF)$,
 149 where $NSAF_x$ and $NSAF_y$ are the summed NSAF values for each protein in sample groups to be compared
 150 ($x = t1$ or $t2$; $y = t0$ or $t1$, respectively) and CF is a correction factor, empirically set to 2 (Tanca et al.,

151 2015, 2012) . Statistical significance of differential protein abundance was further assessed by applying the
152 Student's *t*-test (two-sample comparison, $p < 0.05$) on logarithmic NSAF values, after replacing missing
153 values with 0.1 (empirically determined as in Zybailov et al., 2006) and corrected by using false discovery
154 rate (FDR) as a multiple hypothesis testing, with $FDR < 0.1$ as a threshold limit. Only proteins with $R_{NSAF} >$
155 0.5 or < -0.5 were considered. The mass spectrometry proteomics data have been deposited to the
156 ProteomeXchange Consortium via the PRIDE partner repository with the dataset identifier PXD011059
157 (Deutsch et al., 2017; Sanchez et al., 2015; Vizcaíno et al., 2016) and are reported in Ghisaura et al., 2019.

158

159 **2.5. Multivariate data statistical analysis**

160 Multivariate statistical data analyses (MVDA) were made using SIMCA-P 13.0 version (Umetrics, Inc.,
161 Kinnelon, NJ). Prior to analysis, NSAF values were subjected to log transformation and Pareto scaling. For
162 multivariate preliminary inspection, an unsupervised principal component analysis (PCA) was performed,
163 followed by supervised OPLS-DA (orthogonal partial-least square discriminant analysis) to display as score
164 plot the NSAF clustering, according to each temperature variation. Goodness of all MVA models was
165 evaluated by the cumulative $R^2(\text{cum})$ and the predictive $R^2Y(\text{cum})$ and $Q^2(\text{cum})$ parameters, calculated
166 according to the cross-validation method. In particular, $R^2Y(\text{cum})$ is defined as the proportion of variance in
167 the data explained by the models and indicates the goodness of fit, whereas $Q^2(\text{cum})$ is defined as the
168 proportion of variance in the data predictable by the model. Both $R^2Y(\text{cum})$ and $Q^2(\text{cum})$ vary between 0
169 and 1: a good prediction model is indicated by $Q^2(\text{cum}) > 0.5$, whereas a $Q^2(\text{cum}) > 0.8-0.9$ means an
170 excellent predictive ability of the model; for $Q^2(\text{cum})$ values close to 0.5, no statistical group separation
171 between observed clusters was considered (Westerhuis et al., 2008).

172

173 **2.6. Pathway analysis**

174 Gene ontology and protein annotations were retrieved from UniProtKB (<http://www.uniprot.org>). The
175 uncharacterized sequences were blasted on NCBI non-redundant database:
176 (<http://blast.ncbi.nlm.nih.gov/Blast.cgi>) to find the homologous proteins. For pathway analysis two online
177 software packages were used: STRING version 10 (Search Tool for the Retrieval of Interacting
178 Genes/Proteins; <http://string-db.org>) (Szklarczyk et al., 2017) and the online software package IPA (version

179 9.0; Ingenuity Systems, Redwood City, CA). For STRING, an enrichment analysis was performed with all
180 differentially expressed proteins, and KEGG pathways, GO Biological Processes and GO Molecular
181 Functions implemented in the web platform were investigated by using the *Danio rerio* as organism model.
182 Only the pathways and molecular networks displaying an FDR < 0.05 were considered as significantly
183 enriched in the protein list and were considered for further analyses. For IPA analysis, since the software
184 operates on a database built on the literature generated for humans and rodents, fish UniProt IDs were
185 replaced with the closest mouse (*Mus musculus*) protein equivalents to enable a wider knowledge-based
186 investigation of pathways as previously described (Addis et al., 2011; Ghisaura et al., 2014; Terova et al.,
187 2014), being this a larger and better investigated database. The list of protein identifications (IDs), with
188 their respective R_{NSAF} and p values (< 0.05) were used for the gene ontology analysis. Diseases and
189 functions were specifically considered to focus on the physiological and health state of the fish liver during
190 cold treatment.

191

192 3. Results and Discussion

193

194 3.1. Cooling phase

195 A preliminary evaluation of experimental NSAF data with PCA indicated that liver proteomes at t1 were
196 clearly separated from those at t0 (**Figure S1**). This result was confirmed by a further supervised approach
197 based on OPLS-DA (**Figure 1a**). Indeed, the OPLS-DA model showed a very good fit parameter ($R^2Y(cum)$
198 = 0.819) and a fairly good prediction ability ($Q^2(cum) = 0.828$), as shown by the model validation results
199 (**Figure 1**).

200 A total of 42 proteins showed statistically significant differences in abundance at t1 vs t0 ($R_{NSAF} > 0.5$ or <
201 -0.5 , $p < 0.05$, FDR < 0.1) and are listed in **Table 1**. According to STRING, numerous metabolic pathways
202 were affected, as reported in **Table S1**. KEGG pathways were mainly related to carbon metabolism such as
203 amino acid metabolism, including the phenylalanine, tyrosine and cysteine and methionine metabolisms.
204 Other general pathways that encompass metabolic pathways and carbon metabolism were also statistically
205 significant (FDR < 0.05). Amino acid metabolism plays an important role in fish metabolism for protein
206 synthesis, glucose formation, and energy. For example, Costas et al, (2011) observed increased levels of

207 amino acids and other metabolites during long term feed deprivation in Senegalese sole fish, and amino acids
208 are considered the major source of energy in this carnivorous fish species. Feed deprivation led to active
209 gluconeogenic active processes in the liver supported by proteolysis in 21 days feed-deprived sole,
210 suggesting that amino acids are employed as a carbon source for gluconeogenesis for the maintenance of
211 plasma glucose levels. Phenylalanine and tyrosine can influence pigmentation, development, feed intake,
212 growth performance, immunity, and survival of fish in the natural environment. Tyrosine synthesized from
213 the essential amino acid phenylalanine is a precursor for important hormones and neurotransmitters,
214 including thyroid hormones that play an important role next to energy metabolism and protein synthesis
215 (Jasour et al., 2017; Li et al., 2009).

216 According to IPA, increased proteins were mainly associated to cellular stress and to protein and lipid
217 degradation processes, while decreased proteins were mostly related to protein synthesis, actin-binding
218 activity, amino acid metabolism, and protection from oxidative stress (**Table S2**). Several enzymes included
219 in amino acid metabolism showed significant changes. An increase in fumarylacetoacetase and a reduction in
220 4-hydroxyphenylpyruvate dioxygenase were observed (**Table 1**), both enzymes being involved in the
221 catabolism of phenylalanine and tyrosine. Downregulation of phenylalanine and tyrosine catabolism has
222 been associated to liver damage (Richard et al., 2016), confirming the key role of these amino acids in the
223 physiological response of sea bream to cold challenge. Catabolism of specific amino acids, including
224 tyrosine and phenylalanine through homogentisate 1,2-dioxygenase, was also observed to be reduced under
225 cold stress by Ibarz and coworkers (2010a). This has been associated to the possible entrance of tyrosine and
226 phenylalanine in the TCA cycle to produce energy. Likely, it has been suggested that high dietary
227 availability of amino acids, methyl donors (betaine, choline) and cofactors (folate) supports the flux toward
228 the methionine cycle thus favoring optimal homeostasis, helping fish to cope with exogenous stress and
229 finally improving feed performance (Richard et al., 2016). Amino acids can be considered an important
230 glucogenic source in fish. In this regard, high inclusion levels of feathermeal in feed have been correlated
231 with hepatic levels of leucine, isoleucine, tyrosine, valine, methionine, arginine, and phenylalanine involved
232 in energy metabolism. Moreover, an increased concentration of these amino acids in the liver was observed
233 in the same study, indicating their inhibition from entering the TCA metabolic pathway to generate energy
234 (Jasour et al., 2017). Formimidoyltransferase-cyclodeaminase was also increased. This enzyme is involved in

235 the sub-pathway that synthesizes glutamate by means of histidine degradation and tetrahydrofolate
236 conversion in the pathway of one carbon metabolism. Thioredoxin and metallothionein were reduced. These
237 proteins act as primary liver defense under oxidant attack at low temperatures. Their reduction might be
238 associated to loss of hepatic functionality under cold stress (liver failure), confirming that oxidative stress
239 and amino acid metabolisms are the pathways mainly affected by cold. Previous results by Ibarz et al.
240 (2010a) are in line with our findings. In their proteomic study on gilthead sea bream liver under acute cold
241 challenge, they identified oxidative stress, amino acid metabolisms and carbohydrate metabolism as the most
242 perturbed pathways.

243 Actin-related proteins such as cofilin-2 were reduced during water cooling. Similarly, Ibarz and coworkers
244 (2010a) found decreased actin levels in cold-stressed fish. Both alpha and beta tubulins, the components of
245 cytoskeletal microtubules, were increased, as already observed in previous studies on cold challenged
246 gilthead sea breams. The same authors suggested that tubulin has a protective effect against cold stress, but
247 the exact mechanisms are still under study. The evident increase seen in proteasome-associated proteins,
248 together with the observed changes in cytoskeletal proteins, might suggest the occurrence of tissue
249 remodeling processes induced by thermal stress. A reduction in heart-like FABP or FABP3 was observed
250 (**Table 1**). Mininni and coworkers (2014) reported several changes in FABP isoforms according to
251 transcriptomics, but did not report changes in FABP3.

252 Several “diseases and functions” categories were also significant according to IPA (**Table S2**). These results,
253 although obtained by comparison of literature based on mouse, support the finding that the most relevant
254 changes in liver metabolism occurred during the cooling phase. As summarized in **Table S2**, it is worth
255 noting that several significantly modified proteins were involved in cellular growth and proliferation,
256 inflammatory response, and infectious diseases. This may suggest some similarity with the well-known
257 effects of winter syndrome in gilthead sea bream (Ibarz et al., 2010b).

258

259 **3.2. Cold maintenance phase**

260 In the cold maintenance phase (constant 11°C, comparison t2 vs t1), liver proteins showed less marked
261 changes than in the cooling phase. Consequently, the t2 and t1 sample clusters displayed a lower PCA
262 separation (**Figure S1b**). Quantitative estimation of discriminative values of the model is given by lower

263 Q2(cum) index ($Q2(\text{cum}) = 0.55$), close to the threshold limit for a biological model discrimination
264 (Westerhuis et al., 2008). Similarly, the goodness of fit of the related OPLS-DA model led to a lower
265 Q2(cum) value ($Q2(\text{cum})_{\text{COLDMAINT}} = 0.69$, **Figure 2**) when compared to the cooling phase ($Q2(\text{cum})_{\text{COOLING}}$
266 $= 0.83$, **Figure 1**). These observations indicate a lower prediction ability of all the MVDA models associated
267 to the cold maintenance phase vs the cooling phase, and suggest that t2 and t1 (that is, along cold
268 maintenance) are more similar to each other (**Figure S1b**) than t0 and t1 (beginning and end of cooling
269 phase).

270 In this case, only 24 significantly differential proteins were identified in all samples ($R_{\text{NSAF}} > 0.5$ or < -0.5 , $p <$
271 0.05 , $\text{FDR} < 0.1$) and are listed in **Table 2**. Several proteins were associated to the methionine cycle, such as
272 betaine-homocysteine-S-methyltransferase (BHMT). Interestingly, this protein underwent the most intense
273 change in abundance observed in the whole study ($R_{\text{NSAF}} = 2.96$). Other proteins with ribosomal activity,
274 glycolytic and gluconeogenic function, were increased in t2 vs t1, whereas proteins associated to scavenger
275 activity, migration and cellular organization, protein transport and proteolysis, adenosine and homocysteine
276 synthesis were decreased (**Table S1**).

277 Enrichment analysis indicated the main KEGG pathways altered during the cold maintenance phase (**Table**
278 **S1**). Among them, the categories metabolic pathways and glycolysis/gluconeogenesis had three molecules
279 involved. Amino acid metabolisms, including alanine, aspartate and glutamate metabolism, cysteine and
280 methionine metabolisms, were also significant, confirming the key role of energy metabolism and of the
281 methionine cycle. KEGG pathways, GO Biological Processes, and GO Molecular functions are fully detailed
282 in **Table S1**. Only two diseases and function features were associated to the cold maintenance phase (**Table**
283 **S2**), supporting the above observations.

284 In a previous investigation on the metabolic response of sea breams to low water temperatures (Melis et al.,
285 2017), liver gluconeogenesis was more affected than glycolysis during constant cold temperatures. In this
286 study, an increased abundance of proteins implicated in carbohydrate metabolism was observed in the same
287 conditions. Also, the observed perturbation of amino acid metabolism during the cold maintenance phase is
288 confirmed by previous proteomic investigations (Richard et al., 2016). In particular, the methionine cycle
289 and several related molecules (betaine, choline/phosphocholine and glutathione) were found to be affected
290 during prolonged exposure to low temperatures. Several scientific reports on cold challenged gilthead sea

291 bream highlight a methionine cycle activation under stress conditions (Ibarz et al., 2010; Mininni et al.,
292 2014; Richard et al., 2016). Amino acid interconversion and catabolism processes, often resulting in
293 upregulation of BHMT, are likely triggered during cold stress to prevent hepatic accumulation of cytotoxic
294 molecules such as homocysteine. However, although fast water temperature decrease such as 20°C to 8°C in
295 3 days (Ibarz et al., 2010a) can lead to downregulation of BHMT, slower cooling conditions seem to
296 consistently result in an increased expression. Our previous work (Melis et al., 2017), based on a first gradual
297 temperature decrease followed by a cold maintenance phase, reached a similar conclusion, i.e. adjustments of
298 methionine cycle metabolism are activated during prolonged stress while they are not observed during the
299 first, more acute phases of temperature decrease. In this sense, BHMT appears as a key proteomic regulator
300 throughout a persistent stressful condition, acting via antioxidant mechanisms by balancing S-adenosyl-
301 methionine and preventing toxic homocysteine accumulation. The increase in BHMT was also associated to
302 an unbalanced amino acid composition of diets leading to increased oxidative stress (Ghisaura et al., 2014),
303 which suggests that BHMT is a good indicator related to general fish homeostasis. The changes in BHMT
304 levels might therefore be related also to glutathione biosynthesis, reflecting a different extent of oxidative
305 stress caused on hepatocytes by the different temperatures; more specifically, its increase in the cold
306 maintenance phase (t2 vs t1) indicates that a higher oxidative stress is exerted by long exposure to winter
307 temperatures (Ghisaura et al., 2014). Other amino acid degradation pathways and changes in proteins mainly
308 implicated in stress response and cellular defense were represented by Adenosylhomocysteinase (AHCY or
309 SAM) that is involved in the superpathway of methionine degradation, as well as in the methionine salvage
310 pathway; specifically, it catalyzes the reversible hydrolysis of S-adenosylhomocysteine to adenosine and L-
311 homocysteine and has a central role in the regulation of methyltransferase reactions, important for liver
312 homeostasis maintenance (Ghisaura et al., 2014). As pointed out by Richard et al., (2016) its deficiency is
313 usually associated with hepatic damages.

314 Increased purine metabolism also plays a crucial role in facing cold stress. Its involvement was observed in
315 both muscle and liver of gilthead sea bream during cold maintenance phases by metabolomics (Melis et al.,
316 2017) and was confirmed here by the observed increase in purine nucleoside phosphorylase-like (PNP). It
317 was also postulated that the involvement of purine metabolism pathways in cold challenged gilthead sea

318 bream might be somewhat associated to other symptoms of the winter syndrome, such as skin pigmentation
319 and immune suppression (Melis et al., 2017).

320

321 3.3. Overall changes

322 Proteomic profiles at the starting time (t0) were then compared with those at the end of the trial (t2) to gain a
323 general overview of the changes occurring along prolonged thermal stress. A very clear separation of the two
324 conditions was highlighted by the PCA score plot (**Figure S1c**) showing a $Q^2(\text{cum}) = 0.68$. Furthermore,
325 OPLS-DA score plot and related model validation (**Figure 3**) showed an excellent cluster separation with a
326 $Q^2(\text{cum})$ closer to 0.9 ($Q^2(\text{cum}) = 0.885$), which implies a higher goodness of discrimination with respect to
327 both t1/t0 (**Figure 1**) and t2/t1 (**Figure 2**).

328 In this case, 59 proteins showed differences in abundance ($R_{\text{NSAF}} > 0.5$ or < -0.5 , $p < 0.05$, $\text{FDR} < 0.1$) and
329 are listed in **Table 3**. Proteins related to proteolysis processes, energy conversion, carbohydrate and amino
330 acid metabolism and mitochondrial activity were increased, while those involved in fatty acid metabolism
331 and amino acid conversion were decreased, as well as proteins associated to protection from oxidative stress
332 and purine degradation (**Table S1**). Several stress-driven metabolic changes were observed. Abundance
333 variations affected proteins involved in the metabolism of key amino acids (histidine, alanine, aspartate and
334 glutamate; tyrosine, phenylalanine, arginine and proline; cysteine and methionine). Full KEGG pathways,
335 GO Biological Processes and GO Molecular functions are detailed in **Table S1**. The categories pyruvate
336 metabolism and starch and sucrose metabolisms were also involved. Moreover, five significantly increased
337 diseases and functions categories were represented by inflammatory responses of the organism, generation of
338 reactive oxygen species (and related free radical scavenging functions), liver necrosis, lipid metabolisms and
339 their oxidation (functional to energy production) (**Table S2**).

340 The analysis of the overall cold challenge confirmed the observations done on the two separate phases
341 (cooling and cold maintenance). Upon constant temperature decrease, proteins implicated in proteolysis,
342 lipolysis, glycolysis and glycogenolysis, together with those implicated in amino acid metabolism, increased
343 in abundance, possibly to intensify energy production during cold stress. In fact, as seen in many studies
344 (Chang et al., 2018; Ibarz et al., 2010b, 2010a; Richard et al., 2016), there is a strong mobilization of
345 extrahepatic fat deposits to liver and glycogen reserves. Amino acid degradation pathways (phenylalanine

346 and tyrosine catabolism) and changes in proteins mainly implicated in stress response and cellular defense
347 were represented by a slightly lowered uricase (**Table 3**), that catalyzes the oxidation of uric acid to 5-
348 hydroxyisourate and then to allantoin, a degradation product of purine nucleobases. **Table S2** reports
349 diseases and functions categories affected by cold stress exposure. Cold mainly affected inflammatory and
350 organ damage processes, oxidative stress response and tyrosine degradation. The involvement of this latter
351 pathway was recently confirmed by our research group using ^1H NMR-based metabolic fingerprinting (Melis
352 et al., 2017) and by Richard and coworkers (Richard et al., 2016) who specifically described phenylalanine
353 and tyrosine catabolism and their interconversion in the proteomic response of gilthead sea bream to low
354 temperature.

355

356 **4. Conclusions**

357 The protein makeup of sea bream liver undergoes several changes upon exposure to decreasing water
358 temperature, suggesting the occurrence of a metabolic shift enabling adaptation to changed environmental
359 conditions. This shift occurs mainly along temperature lowering in a cold adaptation phase. The maintenance
360 of low but constant temperatures seems to affect protein levels to a lesser extent, although significant
361 changes emerge also in this phase, such as in methionine metabolism. Gaining a greater knowledge of sea
362 bream metabolic changes to cold adaptation might be of use to fish farmers for the development of specific
363 aquaculture practices aimed at mitigating the negative effects of cold on fish growth, including the design of
364 novel feed formulations for the winter season.

365

366 **Acknowledgements**

367 The PRIDE team is acknowledged for the support for MS data deposition into ProteomeXchange
368 Consortium (<http://proteomecentral.proteomexchange.org>) (identifier PXD011059). This work has been
369 funded by Sardinia Regional Government by means of Sardegna Ricerche (art. 26 L.R. 37/98). The authors
370 are grateful to Dr. Roberto Cappuccinelli for conducting growth trials and Dr. Elia Bonaglini for technical
371 assistance in growth experiments and during sampling. The constant and valuable support of Tonina Roggio
372 is also gratefully acknowledged.

373 **Table 1**

374

375 Sea bream liver proteins undergoing significant changes during the cooling phase (t1 vs t0). $R_{NSAF} >$
376 0.5 or < -0.5 ; p value < 0.05 ; FDR multiple comparison test < 0.1 .

377

Accession number	Protein name	$R_{NSAF} t1/t0$
<i>Increased proteins</i>		
Q4RBW9	Proteasome subunit beta type-2	2.0501
B3F9U6	Hemoglobin beta chain	1.7291
Q1PCB2	Beta globin	1.6826
P86232	Ezrin (Fragments)	1.5108
P11748	Hemoglobin subunit alpha	1.3526
K7GAK5	Tubulin beta-7 chain	0.9969
Q4S3J3	GTP-binding nuclear protein Ran	0.8656
Q91060	Tubulin alpha chain	0.8281
M9P052	Lysosomal acid lipase	0.8276
Q4RVS0	ATP synthase F(0) complex subunit B1, mitochondrial	0.7537
L5M3T4	GTP-binding protein SAR1a	0.707
Q4S798	Nucleolin isoform X2 (Fragment)	0.6757
H2MYW8	Fumarylacetoacetase	0.6599
J7FII7	Glutathione S-transferase (Fragment)	0.6588
G9I0G6	Transferrin	0.6428
S4S3W7	Phosphoglucomutase 1 (Fragment)	0.5869
I3JSE9	Formimidoyltransferase-cyclodeaminase-like	0.5706
G1QD60	H3 histone (Fragment)	0.5705
H2LS09	Nucleolin isoform X1	0.5106
<i>Decreased proteins</i>		
Q0GPQ8	Cytochrome P450 2P11	-0.5457
A0A060VGE8	Cytochrome oxidase subunit II	-0.5506
W5LDH9	Uricase	-0.584
G3PTX7	Endoplasmic reticulum resident protein 27	-0.5926
H0YZD0	Electron transfer flavoprotein subunit alpha, mitochondrial	-0.6356
W5N925	Protein disulfide-isomerase (Fragment)	-0.6434
H2RKV3	Malic enzyme	-0.6595
M4AX90	Peroxisomal 2,4-dienoyl-CoA reductase-like	-0.6643
Q27HS3	Vascular smooth muscle alpha-actin (Fragment)	-0.6784
Q4RKE4	Fatty acid-binding protein, heart-like	-0.7223
Q8JHC5	Metallothionein (Fragment)	-0.7259
F1Q6E1	4-hydroxyphenylpyruvate dioxygenase	-0.7963
A0A060WA9	Adenosylhomocysteinase B	-0.8248
M4VQF0	Glyceraldehyde-3-phosphate dehydrogenase	-0.8662
M4AAN9	Phosphate carrier protein, mitochondrial-like isoform X1	-0.8739
F7DQ24	11-cis retinol dehydrogenase-like	-0.92
F7FYK5	40S ribosomal protein SA-like	-1.0889
A0A060YQH0	Aspartate aminotransferase, cytoplasmic-like	-1.1398
B5X8Y0	Cofilin-2	-1.2505
H2VEH5	Peptidyl-prolyl cis-trans isomerase	-1.2816
B9EN58	Thioredoxin	-1.841
G3HK42	60S ribosomal protein L30	-2.441
G3UYV7	40S ribosomal protein S28 (Fragment)	-2.7022

378

379 **Table 2**
 380
 381 Sea bream liver proteins undergoing significant changes during the maintenance phase (t2 vs t1).
 382 $R_{NSAF} > 0.5$ or < -0.5 ; p value < 0.05 ; FDR multiple comparison test < 0.1 .
 383

Accession number	Protein name	R_{NSAF} t2/t1
<i>Increased proteins</i>		
I3KAP1	Betaine-homocysteine S-methyltransferase 1-like	2.9636
E9QBF0	Triosephosphate isomerase	1.4764
M7BNB0	60S ribosomal protein L30	1.4457
P61155	40S ribosomal protein S19	1.4016
F6Q602	Probable imidazolonepropionase	1.3571
C1KBH6	Phosphoenolpyruvate carboxykinase	1.3021
H2L7M4	Keratin, type I cytoskeletal 18-like	1.1887
F1QXV8	Phosphoglycerate kinase	1.0446
W5LXZ1	Purine nucleoside phosphorylase-like (Fragment)	0.9842
H2MFC0	Obg-like ATPase 1	0.9796
M4ANE8	Glutamate dehydrogenase, mitochondrial-like	0.766
G3Q9K3	ATP synthase subunit gamma	0.7505
C3KIP4	Myosin light polypeptide	0.7423
B5X124	Deoxyribose-phosphate aldolase	0.6882
I3KYC9	Fumarate hydratase, mitochondrial-like	0.6618
F1R0A9	Glucose-6-phosphate translocase isoform X1	0.5549
<i>Decreased proteins</i>		
M9NZ74	94 kDa glucose-regulated protein	-0.5354
L5M3T4	GTP-binding protein SAR1a	-0.6744
Q4QY80	Elastase 4-like protein (Fragment)	-0.9622
H2UYH6	60S ribosomal protein L6-like	-1.0566
H3CCF6	Delta-1-pyrroline-5-carboxylate dehydrogenase, mitochondrial	-1.1152
G5DYL0	Putative s-adenosylhomocysteine hydrolase (Fragment)	-1.294
H7C3T4	Peroxiredoxin-4 (Fragment)	-1.366
P86232	Ezrin	-1.4512

384
 385

386
387
388
389
390**Table 3**Sea bream liver proteins undergoing significant changes along the whole trial (t2 vs t0). $R_{NSAF} > 0.5$ or < -0.5 ; p value < 0.05 ; FDR multiple comparison test < 0.1 .

Accession number	Protein name	R_{NSAF} t2/t0
<i>Increased proteins</i>		
S7MY91	60S ribosomal protein L12	2.434
Q4RBW9	Proteasome subunit beta type-2	2.1625
Q1PCB2	Beta globin	1.8357
P56251	Hemoglobin subunit beta	1.6591
P11748	Hemoglobin subunit alpha	1.5843
E9QH32	Nucleoside diphosphate kinase	1.5778
M4ABN8	Mitochondrial pyruvate carrier 2-like	1.463
F2YLA1	Transferrin	1.1602
H2V638	Profilin	1.0975
H2U0L4	Mitochondrial 2-oxodicarboxylate carrier	1.0443
H0VMR9	Histone H2B	1.023
K7GAK5	Tubulin beta-7 chain	0.9934
E9QBF0	Triosephosphate isomerase	0.9793
M4AJN9	L-2-hydroxyglutarate dehydrogenase, mitochondrial-like	0.9785
B5XDR2	Inorganic pyrophosphatase 2, mitochondrial	0.7825
H2MWN8	Formimidoyltransferase-cyclodeaminase	0.7612
H2LS09	nucleolin isoform X1	0.7608
H2L7M4	Keratin, type I cytoskeletal 18-like	0.7579
C4PAW7	Microsomal epoxide hydrolase	0.7529
I3KYC9	Fumarate hydratase, mitochondrial-like	0.7459
I3JD93	40S ribosomal protein S25-like	0.718
M4ANE8	Glutamate dehydrogenase, mitochondrial-like	0.7107
A0A060Z139	Ubiquitin-like modifier-activating enzyme 1	0.6808
Q9HAP1	Valosin-containing protein (Fragment)	0.6602
F1R0A9	Glucose-6-phosphate translocase isoform X1	0.6311
H2MNV5	Tubulin beta-1 chain	0.6074
G3Q9Y8	Clathrin heavy chain 1 isoform X2	0.5594
Q4S798	nucleolin isoform X2	0.5317
F6Y7A5	Aldehyde dehydrogenase family 8 member A1 isoformX1	0.5194
K7FFD9	Delta-1-pyrroline-5-carboxylate dehydrogenase, mitochondrial	0.5045
<i>Decreased proteins</i>		
E6ZHH2	Catechol-O-methyltransferase domain-containing protein 1	-0.5385
G3NRH9	Transketolase	-0.5529
H2RKV3	Malic enzyme	-0.5545
Q0GPQ8	Cytochrome P450 2P11	-0.5905
E9L835	Beta actin-1	-0.5967
H2L6X3	Urocanate hydratase	-0.6063
G3PTX7	Endoplasmic reticulum resident protein 27	-0.6394
D3TJK0	Alpha-amylase	-0.6405
W5N925	Protein disulfide-isomerase (Fragment)	-0.7119
M4AX90	Peroxisomal 2,4-dienoyl-CoA reductase-like	-0.7159
M9P0A8	Catalase	-0.7396
Q6USB8	Glutathione S-transferase (Fragment)	-0.8419
H2TY77	Carboxypeptidase A1-like	-0.8624
Q4QY80	Elastase 4-like protein (Fragment)	-0.8795

Q8JHC5	Metallothionein (Fragment)	-0.8796
F1Q6E1	4-hydroxyphenylpyruvate dioxygenase	-0.8941
M4AAN9	Phosphate carrier protein, mitochondrial-like isoform X1	-0.9372
K4GAL6	Adenosylhomocysteinase	-0.9525
F7DQ24	11-cis retinol dehydrogenase-like, partial	-0.9856
W5LDH9	Uricase	-1.0609
R0LYE9	Maleylacetoacetate isomerase (Fragment)	-1.0864
F7FYK5	40S ribosomal protein SA-like	-1.1605
B5X3S0	Estradiol 17-beta-dehydrogenase 12-B	-1.1615
M9P0N9	Heart-type fatty acid binding protein	-1.1928
A0A060YQH0	Aspartate aminotransferase, cytoplasmic-like	-1.2149
S9XSM0	Actin, cytoplasmic 2	-1.26
P81399	Fatty acid-binding protein 1, liver	-1.336
H2VEH5	Peptidyl-prolyl cis-trans isomerase	-1.3479
B5X8Y0	Cofilin-2	-1.7414

391

392 **Figure captions**393 **Fig. 1.**

394 **OPLS-DA score plot based on the NSAF values of liver proteins observed during the cooling phase**
395 **(t1/t0).** Cross-validation parameters R2X (cum), R2Y (cum) and Q2 (cum) are reported. The ellipse
396 represents T2 Hotelling's plot with 95% confidence.

397

398 **Fig. 2.**

399 **OPLS-DA score plot based on the NSAF values of liver proteins observed during the cold maintenance**
400 **phase (t2/t1).** Cross-validation parameters R2X (cum), R2Y (cum) and Q2 (cum) are reported. The ellipse
401 represents T2 Hotelling's plots with 95% confidence.

402

403 **Fig. 3.**

404 **OPLS-DA score plot based on on the NSAF values of liver proteins undergoing abundance changes**
405 **along the cooling trial (t2/t0).** Cross-validation parameters R2X (cum), R2Y (cum) and Q2 (cum) are
406 reported. The ellipse represents T2 Hotelling's plots with 95% confidence.

407

408 **References**

- 409 Abram, Q.H., Dixon, B., Katzenback, B.A., 2017. Impacts of low temperature on the teleost immune system.
410 *Biology* (Basel). 6, 39. <https://doi.org/10.3390/biology6040039>
- 411 Addis, M.F., 2013. Proteomics in Foods, in: Toldrá, F., Nollet, L.M.L. (Eds.), *Proteomics in Foods:*
412 *Principles and Applications*. Springer US, Boston, MA, pp. 181–203. [https://doi.org/10.1007/978-1-](https://doi.org/10.1007/978-1-4614-5626-1)
413 [4614-5626-1](https://doi.org/10.1007/978-1-4614-5626-1)
- 414 Addis, M.F., Cappuccinelli, R., Tedde, V., Pagnozzi, D., Porcu, M.C., Bonaglini, E., Roggio, T., Uzzau, S.,
415 2010a. Proteomic analysis of muscle tissue from gilthead sea bream (*Sparus aurata*, L.) farmed in
416 offshore floating cages. *Aquaculture* 309, 245–252. <https://doi.org/10.1016/j.aquaculture.2010.08.022>
- 417 Addis, M.F., Cappuccinelli, R., Tedde, V., Pagnozzi, D., Viale, I., Meloni, M., Salati, F., Roggio, T., Uzzau,
418 S., 2010b. Influence of *Moraxella* sp. colonization on the kidney proteome of farmed gilthead sea
419 breams (*Sparus aurata*, L.). *Proteome Sci.* 8, 50. <https://doi.org/10.1186/1477-5956-8-50>
- 420 Addis, M.F., Pisanu, S., Ghisaura, S., Pagnozzi, D., Marogna, G., Tanca, A., Biosa, G., Cacciotto, C.,
421 Alberti, A., Pittau, M., Roggio, T., Uzzau, S., 2011. Proteomics and pathway analyses of the milk fat
422 globule in sheep naturally infected by *Mycoplasma agalactiae* provide indications of the in vivo
423 response of the mammary epithelium to bacterial infection. *Infect. Immun.* 79, 3833–3845.
424 <https://doi.org/10.1128/IAI.00040-11>
- 425 Alves, R.N., Cordeiro, O., Silva, T.S., Richard, N., de Vareilles, M., Marino, G., Di Marco, P., Rodrigues,
426 P.M., Conceição, L.E.C., 2010. Metabolic molecular indicators of chronic stress in gilthead seabream
427 (*Sparus aurata*) using comparative proteomics. *Aquaculture* 299, 57–66.
428 <https://doi.org/10.1016/j.aquaculture.2009.11.014>
- 429 Braceland, M., Bickerdike, R., Tinsley, J., Cockerill, D., McLoughlin, M.F., Graham, D. a, Burchmore, R.J.,
430 Weir, W., Wallace, C., Eckersall, P.D., 2013. The serum proteome of Atlantic salmon, *Salmo salar*,
431 during pancreas disease (PD) following infection with salmonid alphavirus subtype 3 (SAV3). *J.*
432 *Proteomics* 94, 423–36. <https://doi.org/10.1016/j.jprot.2013.10.016>
- 433 Brunt, J., Hansen, R., Jamieson, D.J., Austin, B., 2008. Proteomic analysis of rainbow trout (*Oncorhynchus*
434 *mykiss*, Walbaum) serum after administration of probiotics in diets. *Vet. Immunol. Immunopathol.* 121,
435 199–205. <https://doi.org/10.1016/j.vetimm.2007.09.010>
- 436 Chang, C.H., Huang, J.J., Yeh, C.Y., Tang, C.H., Hwang, L.Y., Lee, T.H., 2018. Salinity effects on strategies
437 of glycogen utilization in livers of euryhaline milkfish (*Chanos chanos*) under hypothermal stress.
438 *Front. Physiol.* 9, 81. <https://doi.org/10.3389/fphys.2018.00081>
- 439 Choi, H., Nesvizhskii, A.I., 2008. False Discovery Rates and Related Statistical Concepts in Mass
440 Spectrometry-Based Proteomics. *J. Proteome Res.* 7, 47–50. <https://doi.org/10.1021/pr700747q>
- 441 Contessi, B., Volpatti, D., Gusmani, L., Galeotti, M., 2006. Evaluation of immunological parameters in
442 farmed gilthead sea bream, *Sparus aurata* L., before and during outbreaks of “winter syndrome.” *J. Fish*
443 *Dis.* 29, 683–690. <https://doi.org/10.1111/j.1365-2761.2006.00765.x>
- 444 Costas, B., Aragão, C., Ruiz-Jarabo, I., Vargas-Chacoff, L., Arjona, F.J., Dinis, M.T., Mancera, J.M.,

- 445 Conceição, L.E.C., 2011. Feed deprivation in Senegalese sole (*Solea senegalensis* Kaup, 1858)
446 juveniles: effects on blood plasma metabolites and free amino acid levels. *Fish Physiol. Biochem.* 37,
447 495–504. <https://doi.org/10.1007/s10695-010-9451-2>
- 448 Davis, P.S., 1988. Two occurrences of the gilthead, *Sparus aurata* Linnaeus 1758, on the coast of
449 Northumberland, England. *J. Fish Biol.* 33, 951–951. [https://doi.org/10.1111/j.1095-](https://doi.org/10.1111/j.1095-8649.1988.tb05545.x)
450 [8649.1988.tb05545.x](https://doi.org/10.1111/j.1095-8649.1988.tb05545.x)
- 451 Deutsch, E.W., Csordas, A., Sun, Z., Jarnuczak, A., Perez-Riverol, Y., Ternent, T., Campbell, D.S., Bernal-
452 Llinares, M., Okuda, S., Kawano, S., Moritz, R.L., Carver, J.J., Wang, M., Ishihama, Y., Bandeira, N.,
453 Hermjakob, H., Vizcaíno, J.A., 2017. The ProteomeXchange consortium in 2017: supporting the
454 cultural change in proteomics public data deposition. *Nucleic Acids Res.* 45, D1100–D1106.
455 <https://doi.org/10.1093/nar/gkw936>
- 456 Douxfils, J., Mathieu, C., Mandiki, S.N.M., Milla, S., Henrotte, E., Wang, N., Vandecan, M., Dieu, M.,
457 Dauchot, N., Pigneur, L.-M., Li, X., Rougeot, C., Méléard, C., Silvestre, F., Van Doninck, K., Raes, M.,
458 Kestemont, P., 2011. Physiological and proteomic evidences that domestication process differentially
459 modulates the immune status of juvenile Eurasian perch (*Perca fluviatilis*) under chronic confinement
460 stress. *Fish Shellfish Immunol.* 31, 1113–1121. <https://doi.org/10.1016/j.fsi.2011.10.001>
- 461 Gallardo, M.Á., Sala-Rabanal, M., Ibarz, A., Padrós, F., Blasco, J., Fernández-Borràs, J., Sánchez, J., 2003.
462 Functional alterations associated with “winter syndrome” in gilthead sea bream (*Sparus aurata*).
463 *Aquaculture* 223, 15–27. [https://doi.org/10.1016/S0044-8486\(03\)00164-9](https://doi.org/10.1016/S0044-8486(03)00164-9)
- 464 Ghisaura, S., Anedda, R., Pagnozzi, D., Biosa, G., Spada, S., Bonaglini, E., Cappuccinelli, R., Roggio, T.,
465 Uzzau, S., Addis, M.F., 2014. Impact of three commercial feed formulations on farmed gilthead sea
466 bream (*Sparus aurata*, L.) metabolism as inferred from liver and blood serum proteomics. *Proteome Sci.*
467 12, 44. <https://doi.org/10.1186/s12953-014-0044-3>
- 468 Ghisaura, S., Loi, B., Biosa, G., Baroli, M., Pagnozzi, D., Roggio, T., Uzzau, S., Anedda, R., Addis, M.F.,
469 2016. Proteomic changes occurring along gonad maturation in the edible sea urchin *Paracentrotus*
470 *lividus*. *J. Proteomics* 144, 63–72. <https://doi.org/10.1016/j.jprot.2016.05.035>
- 471 Ghisaura, S., Melis, R., Biosa, G., Pagnozzi, D., Slawski, H., Uzzau, S., Anedda, R., Addis, M.F., 2019.
472 Liver proteome dataset of *Sparus aurata* exposed to low temperatures. *Data Br.*
- 473 Ibarz, A., Beltrán, M., Fernández-Borràs, J., Gallardo, M.A., Sánchez, J., Blasco, J., 2007. Alterations in
474 lipid metabolism and use of energy depots of gilthead sea bream (*Sparus aurata*) at low temperatures.
475 *Aquaculture* 262, 470–480. <https://doi.org/10.1016/j.aquaculture.2006.11.008>
- 476 Ibarz, A., Blasco, J., Beltrán, M., Gallardo, M.A., Sánchez, J., Sala, R., Fernández-Borràs, J., 2005. Cold-
477 induced alterations on proximate composition and fatty acid profiles of several tissues in gilthead sea
478 bream (*Sparus aurata*). *Aquaculture* 249, 477–486. <https://doi.org/10.1016/j.aquaculture.2005.02.056>
- 479 Ibarz, A., Fernández-Borràs, J., Blasco, J., Gallardo, M.A., Sánchez, J., 2003. Oxygen consumption and
480 feeding rates of gilthead sea bream (*Sparus aurata*) reveal lack of acclimation to cold. *Fish Physiol.*
481 *Biochem.* 29, 313–321. <https://doi.org/10.1007/s10695-004-3321-8>

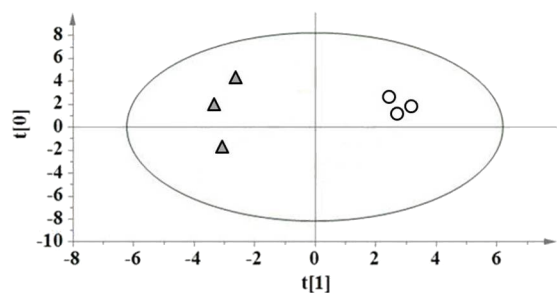
- 482 Ibarz, A., Martín-Pérez, M., Blasco, J., Bellido, D., de Oliveira, E., Fernández-Borràs, J., 2010a. Gilthead sea
483 bream liver proteome altered at low temperatures by oxidative stress. *Proteomics* 10, 963–75.
484 <https://doi.org/10.1002/pmic.200900528>
- 485 Ibarz, A., Padrós, F., Gallardo, M.Á., Fernández-Borràs, J., Blasco, J., Tort, L., 2010b. Low-temperature
486 challenges to gilthead sea bream culture: Review of cold-induced alterations and “Winter Syndrome.”
487 *Rev. Fish Biol. Fish.* 20, 539–556. <https://doi.org/10.1007/s11160-010-9159-5>
- 488 Ibarz, A., Sanahuja, I., Özşahniçlu, I., Eroldogan, O., Sánchez-Nuño, S., Blasco, J., Guerreiro, P.,
489 Fontanillas, R., Fernández-Borràs, J., 2018. Cold-induced growth arrest in gilthead sea bream *Sparus*
490 *aurata*: metabolic reorganisation and recovery. *Aquac. Environ. Interact.* 10, 511–528.
491 <https://doi.org/10.3354/aei00286>
- 492 Isani, G., Andreani, G., Carpenè, E., Di Molfetta, S., Eletto, D., Spisni, E., 2011. Effects of waterborne Cu
493 exposure in gilthead sea bream (*Sparus aurata*): a proteomic approach. *Fish Shellfish Immunol.* 31,
494 1051–8. <https://doi.org/10.1016/j.fsi.2011.09.005>
- 495 Jasour, M.S., Wagner, L., Sundekilde, U.K., Larsen, B.K., Greco, I., Orlien, V., Olsen, K., Rasmussen, H.T.,
496 Hjermitsev, N.H., Hammershøj, M., Dalsgaard, A.J.T., Dalsgaard, T.K., 2017. A comprehensive
497 approach to assess feathermeal as an alternative protein source in aquafeed. *J. Agric. Food Chem.* 65,
498 10673–10684. <https://doi.org/10.1021/acs.jafc.7b04201>
- 499 Käll, L., Storey, J.D., MacCoss, M.J., Noble, W.S., 2008. Assigning significance to peptides identified by
500 Tandem Mass Spectrometry using decoy databases. *J. Proteome Res.* 7, 29–34.
501 <https://doi.org/10.1021/pr700600n>
- 502 Käll, L., Storey, J.D., Noble, W.S., 2009. qvalue: non-parametric estimation of q-values and posterior error
503 probabilities. *Bioinformatics* 25, 964–966. <https://doi.org/10.1093/bioinformatics/btp021>
- 504 Kovacik, A., Tvrda, E., Miskeje, M., Arvay, J., Tomka, M., Zbynovska, K., Andreji, J., Hleba, L.,
505 Kovacikova, E., Fik, M., Cupka, P., Nahacky, J., Massanyi, P., 2018. Trace metals in the freshwater
506 fish *Cyprinus carpio*: effect to serum biochemistry and oxidative status markers. *Biol. Trace Elem. Res.*
507 Jul 2, 1–14. <https://doi.org/10.1007/s12011-018-1415-x>
- 508 Li, P., Mai, K., Trushenski, J., Wu, G., 2009. New developments in fish amino acid nutrition: towards
509 functional and environmentally oriented aquafeeds. *Amino Acids* 37, 43–53.
510 <https://doi.org/10.1007/s00726-008-0171-1>
- 511 Martin, S.A.M., Cash, P., Blaney, S., Houlihan, D.F., 2001. Proteome analysis of rainbow trout
512 (*Oncorhynchus mykiss*) liver proteins during short term starvation. *Fish Physiol. Biochem.* 24, 259–
513 270. <https://doi.org/10.1023/A:1014015530045>
- 514 Melis, R., Sanna, R., Braca, A., Bonaglini, E., Cappuccinelli, R., Slawski, H., Roggio, T., Uzzau, S., Anedda,
515 R., 2017. Molecular details on gilthead sea bream (*Sparus aurata*) sensitivity to low water temperatures
516 from ¹H NMR metabolomics. *Comp. Biochem. Physiol. Part A Mol. Integr. Physiol.* 204, 129–136.
517 <https://doi.org/10.1016/j.cbpa.2016.11.010>
- 518 Mininni, A.N., Milan, M., Ferraresso, S., Petoichi, T., Di Marco, P., Marino, G., Livi, S., Romualdi, C.,

- 519 Bargelloni, L., Patarnello, T., 2014. Liver transcriptome analysis in gilthead sea bream upon exposure
520 to low temperature. *BMC Genomics* 15, 765. <https://doi.org/10.1186/1471-2164-15-765>
- 521 Pagnozzi, D., Biosa, G., Addis, M.F., Mastrandrea, S., Masala, G., Uzzau, S., 2014. An easy and efficient
522 method for native and immunoreactive *Echinococcus granulosus* antigen 5 enrichment from hydatid
523 cyst fluid. *PLoS One* 9, e104962. <https://doi.org/10.1371/journal.pone.0104962>
- 524 Parrington, J., Coward, K., 2002. Use of emerging genomic and proteomic technologies in fish physiology.
525 *Aquat. Living Resour.* 15, 193–196. [https://doi.org/10.1016/S0990-7440\(02\)01172-5](https://doi.org/10.1016/S0990-7440(02)01172-5)
- 526 Richard, N., Silva, T.S., Wulff, T., Schrama, D., Dias, J.P., Rodrigues, P.M.L., Conceição, L.E.C., 2016.
527 Nutritional mitigation of winter thermal stress in gilthead seabream: Associated metabolic pathways
528 and potential indicators of nutritional state. *J. Proteomics* 142, 1–14.
529 <https://doi.org/10.1016/j.jprot.2016.04.037>
- 530 Rodrigues, P.M., Silva, T.S., Dias, J., Jessen, F., 2012. Proteomics in aquaculture: applications and trends. *J.*
531 *Proteomics* 75, 4325–45. <https://doi.org/10.1016/j.jprot.2012.03.042>
- 532 Sanahuja, I., Fernández-Alacid, L., Sánchez-Nuño, S., Ordóñez-Grande, B., Ibarz, A., 2019. Chronic cold
533 stress alters the skin mucus interactome in a temperate fish model. *Front. Physiol.* 9, 1916.
534 <https://doi.org/10.3389/fphys.2018.01916>
- 535 Sánchez-Nuño, S., Sanahuja, I., Fernández-Alacid, L., Ordóñez-Grande, B., Fontanillas, R., Fernández-
536 Borràs, J., Blasco, J., Carbonell, T., Ibarz, A., 2018. Redox challenge in a cultured temperate marine
537 species during low temperature and temperature recovery. *Front. Physiol.* 9, 923.
538 <https://doi.org/10.3389/fphys.2018.00923>
- 539 Sanchez, A., Reisinger, F., Hermjakob, H., Griss, J., Del-Toro, N., Dianes, J.A., Perez-Riverol, Y., Vizcaíno,
540 J.A., Csordas, A., Eisenacher, M., Xu, Q.-W., Ternent, T., Wang, R., Uszkoreit, J., 2015. PRIDE
541 Inspector Toolsuite: moving toward a universal visualization tool for proteomics data standard formats
542 and quality assessment of ProteomeXchange datasets. *Mol. Cell. Proteomics* 15, 305–317.
543 <https://doi.org/10.1074/mcp.o115.050229>
- 544 Spivak, M., Weston, J., Bottou, L., Käll, L., Noble, W.S., 2009. Improvements to the Percolator algorithm
545 for peptide identification from shotgun proteomics data sets. *J. Proteome Res.* 8, 3737–3745.
546 <https://doi.org/10.1021/pr801109k>
- 547 Szklarczyk, D., Morris, J.H., Cook, H., Kuhn, M., Wyder, S., Simonovic, M., Santos, A., Doncheva, N.T.,
548 Roth, A., Bork, P., Jensen, L.J., von Mering, C., 2017. The STRING database in 2017: quality-
549 controlled protein–protein association networks, made broadly accessible. *Nucleic Acids Res.* 45,
550 D362–D368. <https://doi.org/10.1093/nar/gkw937>
- 551 Tanca, A., Biosa, G., Pagnozzi, D., Addis, M.F., Uzzau, S., 2013. Comparison of detergent-based sample
552 preparation workflows for LTQ-Orbitrap analysis of the *Escherichia coli* proteome. *Proteomics* 13,
553 2597–607. <https://doi.org/10.1002/pmic.201200478>
- 554 Tanca, A., Pagnozzi, D., Burrai, G.P., Polinas, M., Uzzau, S., Antuofermo, E., Addis, M.F., 2012.
555 Comparability of differential proteomics data generated from paired archival fresh-frozen and formalin-

- 556 fixed samples by GeLC-MS/MS and spectral counting. *J. Proteomics* 77, 561–576.
557 <https://doi.org/10.1016/j.jpro.2012.09.033>
- 558 Tanca, A., Palomba, A., Pisanu, S., Addis, M.F., Uzzau, S., 2015. Enrichment or depletion? The impact of
559 stool pretreatment on metaproteomic characterization of the human gut microbiota. *Proteomics* 15,
560 3474–3485. <https://doi.org/doi:10.1002/pmic.201400573>
- 561 Terova, G., Pisanu, S., Roggio, T., Preziosa, E., Saroglia, M., Addis, M.F., 2014. Proteomic profiling of sea
562 bass muscle by two-dimensional gel electrophoresis and tandem mass spectrometry. *Fish Physiol.*
563 *Biochem.* 40, 311–322. <https://doi.org/10.1007/s10695-013-9855-x>
- 564 Tort, L., Padrós, F., Rotllant, J., Crespo, S., 1998. Winter syndrome in the gilthead sea bream *Sparus aurata*.
565 Immunological and histopathological features. *Fish Shellfish Immunol.* 8, 37–47.
566 <https://doi.org/10.1006/fsim.1997.0120>
- 567 Varó, I., Navarro, J.C., Rigos, G., Del Ramo, J., Calduch-Giner, J.A., Hernández, A., Pertusa, J.,
568 Torreblanca, A., 2013. Proteomic evaluation of potentiated sulfa treatment on gilthead sea bream
569 (*Sparus aurata* L.) liver. *Aquaculture* 376, 36–44.
- 570 Vilhelmsson, O.T., Martin, S.A.M., Poli, B.M., Houlihan, D.F., 2007. Proteomics: Methodology and
571 Application in Fish Processing, in: *Food Biochemistry and Food Processing*. pp. 401–422.
572 <https://doi.org/10.1002/9780470277577.ch18>
- 573 Vizcaíno, J.A., Csordas, A., Del-Toro, N., Dianes, J.A., Griss, J., Lavidas, I., Mayer, G., Perez-Riverol, Y.,
574 Reisinger, F., Ternent, T., Xu, Q.W., Wang, R., Hermjakob, H., 2016. 2016 update of the PRIDE
575 database and its related tools. *Nucleic Acids Res.* 44, D447–D456. <https://doi.org/10.1093/nar/gkv1145>
- 576 Westerhuis, J.A., Hoefsloot, H.C.J., Smit, S., Vis, D.J., Smilde, A.K., van Velzen, E.J.J., van Duijnhoven,
577 J.P.M., van Dorsten, F.A., 2008. Assessment of PLS-DA cross validation. *Metabolomics* 4, 81–89.
578 <https://doi.org/10.1007/s11306-007-0099-6>
- 579 Westermeier, R., Naven, T., Höpker, H.-R., 2008. *Proteomics in Practice: A Guide to Successful*
580 *Experimental Design*, 2nd Ed. John Wiley & Sons, Ltd.
- 581 Wiśniewski, J.R., Zougman, A., Nagaraj, N., Mann, M., 2009. Universal sample preparation method for
582 proteome analysis. *Nat. Methods* 6, 359–62. <https://doi.org/10.1038/nmeth.1322>
- 583 Zybilov, B., Mosley, A.L., Sardi, M.E., Coleman, M.K., Florens, L., Washburn, M.P., 2006. Statistical
584 analysis of membrane proteome expression changes in *Saccharomyces cerevisiae*. *J. Proteome Res.* 5,
585 2339–47. <https://doi.org/10.1021/pr060161n>
- 586

a

b



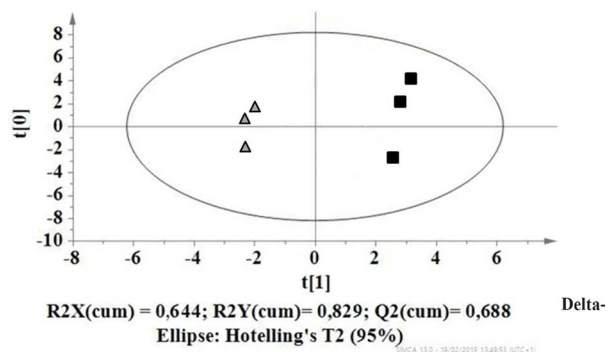
R2X(cum) = 0,349; R2Y(cum) = 0,819; Q2(cum) = 0,828

Ellipse: Hotelling's T2 (95%)

SMCA 13.0 - 15/02/2018 13:49:53 EUPC-1

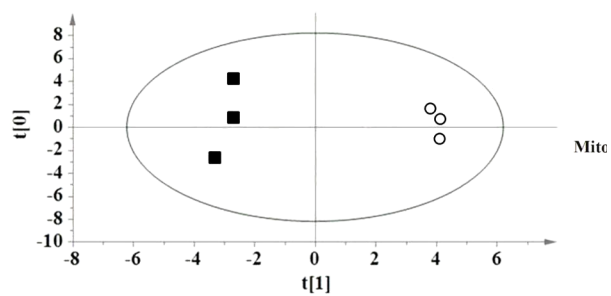
a

b



a

b



R2X(cum) = 0,229; R2Y(cum) = 0,822; Q2(cum) = 0,885
Ellipse: Hotelling's T2 (95%)

1/1/2014 11:01:19 AM 1344933 07/24/14

ACCEPTED MANUSCRIPT

Highlights

- ✓ Exposure to cold temperature modifies the sea bream liver protein abundance profile
- ✓ Proteolysis and aminoacid catabolism are most affected during temperature decrease
- ✓ Methionine cycle and sugar metabolism are most affected upon prolonged cold stress
- ✓ Shotgun proteomics complements the data on hepatic metabolism changes following cold stress